



HAL
open science

The subsonic chemical oxygen-iodine laser : comparison of a theoretical model to experiments in the 30 W range

S. Churassy, A. Bouvier, B. Erba, M. Setra

► To cite this version:

S. Churassy, A. Bouvier, B. Erba, M. Setra. The subsonic chemical oxygen-iodine laser : comparison of a theoretical model to experiments in the 30 W range. *Journal de Physique III*, 1994, 4 (10), pp.2013-2029. 10.1051/jp3:1994254 . jpa-00249239

HAL Id: jpa-00249239

<https://hal.science/jpa-00249239v1>

Submitted on 4 Feb 2008

HAL is a multi-disciplinary open access archive for the deposit and dissemination of scientific research documents, whether they are published or not. The documents may come from teaching and research institutions in France or abroad, or from public or private research centers.

L'archive ouverte pluridisciplinaire **HAL**, est destinée au dépôt et à la diffusion de documents scientifiques de niveau recherche, publiés ou non, émanant des établissements d'enseignement et de recherche français ou étrangers, des laboratoires publics ou privés.

Classification

Physics Abstracts

42.55 — 42.55K — 34.50

The subsonic chemical oxygen-iodine laser : comparison of a theoretical model to experiments in the 30 W range

S. Churassy, A. J. Bouvier, A. Bouvier, B. Erba and M. Setra

Laboratoire de Spectrométrie Ionique et Moléculaire (URA n° 171), CNRS et Université Lyon I,
Bât. 205, 43 Bd du 11 Novembre 1918, 69622 Villeurbanne Cedex, France

(Received 28 February 1994, revised 11 May 1994, accepted 14 June 1994)

Résumé. — Les performances d'un laser subsonique à iode-oxygène chimique à petite échelle ont été améliorées, la puissance laser étant augmentée de 5 W à 34 W avec le même ensemble de pompage. Nous avons montré que, dans ce domaine de puissance, la modélisation du laser doit inclure les effets de température sur les cinétiques des réactions. Notre modèle montre également que l'adjonction d'un gaz tampon tel que SF₆ conduit à un refroidissement important du milieu actif, permettant alors une meilleure extraction de la puissance laser.

Abstract. — The performances of a small scale subsonic chemical oxygen-iodine laser have been improved, the output laser power being increased from 5 to 34 W, with the same gas pumping system. At this power range, we have shown that the modeling of the laser must include the temperature effects on the reaction kinetics. Our model shows also that the addition of a buffer gas such as SF₆ achieves a significant cooling of the active medium, which in turn allows a better laser power extraction.

1. Introduction.

Since the first demonstration of the Chemical Oxygen-Iodine Laser (C.O.I.L.) [1], a number of fundamental studies concerning the characteristics of the laser have been published [2-24]. Extremely high C.W. powers have been obtained in the near infrared region (1.315 μm), 35 kW with a supersonic jet [21a] and more than 600 W in the visible by second harmonic generation [21c]. The unique high power and high brightness of the C.O.I.L. make this laser very attractive for laser-matter interactions. Extremely high efficiency in a subsonic flow was obtained allowing the development of a 1 kW C.W. C.O.I.L. for industrial uses [19, 20a, 21b, 22a, 22b, 24d], and even greater power is forecast with a supersonic C.O.I.L. [24a]. In the above-mentioned C.O.I.L. studies, different models were used to predict the order of magnitude of the output power that should be obtainable with a given set-up. For different reasons, various interactions such as wall deactivations, hyperfine structure [25] or temperature effects were often neglected or else treated only approximately.

Previous studies with a small-scale C.O.I.L. allowed us to establish several aspects of the mechanisms involved in the C.O.I.L. [17] and showed that our modeling of the laser gives predictions in good agreement with experimental results for powers of a few watts.

In this paper we describe several important improvements which have been made, particularly in the cooling of the medium. These techniques have enabled us to increase to C.O.I.L. power from 5 W [17] to 34 W, with the same gas pumping system.

2. Experiment.

The principle of the operation of the laser can be found in the previous references [1-17]. Our laser is of the Bachar-Rosenwaks type [4]. We will describe only the various modifications (Fig. 1) made on our previous set-up [17].

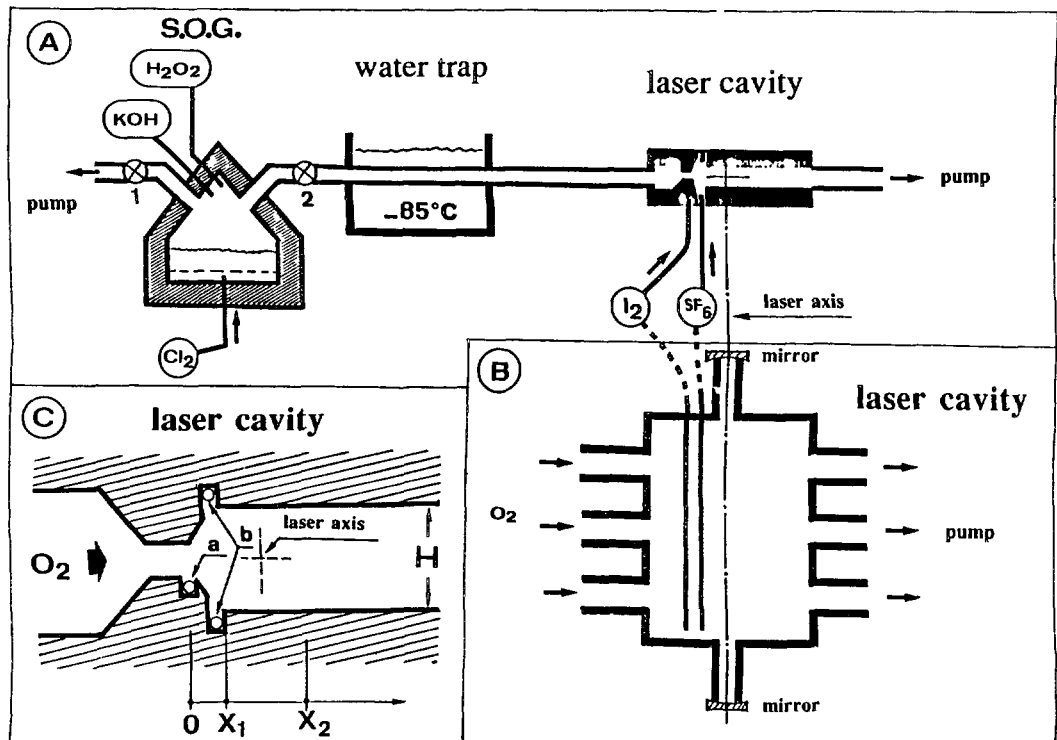


Fig. 1. — Schematics of the experimental set-up: (A) : general view. S.O.G. : Singlet Oxygen Generator of bubbling type, made of P.V.C. material, loaded with 1 liter of H₂O₂ (86 %) and 1 liter of KOH (50 %). 1, 2 : exhausts of the S.O.G. (1 opened and 2 closed during the mixing and cooling of the reactants with a N₂ flow instead of the Cl₂ flow. 2 opened and 1 closed during laser operation). In fact the exhaust 2 is made of 3 glass tubes 5 cm i.d. as shown in the next view. The water trap is made of stainless steel covered with halocarbon wax. (B) : laser cavity, top-view. The active length along the laser axis is 50 cm. Mirrors specifications : diameter 5 cm ; radius of curvature 2 m ; total absorption coefficient $a = a_1 + a_2 = 0.0025$; total transmission coefficient $t = t_1 + t_2 = 0.0050$. The two mirrors are separated by 1.5 m and each of them is protected by a weak Ar flux (not shown in the figure). (C) : laser cavity, cross-section. a : iodine injector, b : SF₆ injectors. X₁, X₂ : active medium limits, as defined by the two mirrors. From the iodine injector position, we have X₁ = 5.3 cm and X₂ = 7.5 cm. The height of the O₂ flow is narrowed to 6 mm just before the iodine injector. In the laser cavity, the height H is 25 mm.

• Following the Watanabe's study [6, 7, 11] which has shown that high flow speeds are incompatible with efficient energy extraction, we have modified the geometry of the laser section. The length of the active medium along the laser cavity axis has been increased from 15 cm to 50 cm and the height H of the gas flow from 15 to 25 mm in order to slow the flow speed from 30 m/s to about 8 m/s.

- The iodine was heated before injection to increase the iodine vapor pressure.
- A new chemical Singlet Oxygen Generator (SOG) was built. The main improvement was the shortening of the different ducts between the SOG and the cavity, and the use of PVC material to decrease the singlet oxygen $O_2(^1\Delta_g)$ (abbreviated as O_2^*) losses in transport. So the O_2^* concentration increased and was of the order of 50 % at the entrance of the laser cavity.
- Several experiments showed that iodine atoms or molecules were quickly adsorbed on the walls along the stream, and even migrated against the gas flow ; O_2^* was deactivated on the walls saturated with iodine. Two alterations were made. First the cavity was strongly narrowed before the iodine injection (from 20-25 mm to 6 mm) to avoid the iodine reflux. Secondly, a flow of a heavy and inert gas (SF_6) was introduced (Fig. 1) mainly to decrease the reactive gas temperature. In the absence of SF_6 and with 2.8×10^{-3} mole/s of Cl_2 and 0.8-0.9 Torr pressure, we obtained a maximum laser power of 18 W. This power increases to 30 W when SF_6 is added. The O_2^* concentration was measured as before [17].

In all the experiments, the laser beam has been found to be uniform in power density in any cross-section. Such uniformity can be obtained only if a very high number of transverse modes are present in the laser resonator. This, in turn, requires that the resonator has a large Fresnel number $N = a^2/\ell\lambda$, where a is the output diameter, ℓ the mirror separation and λ the laser wavelength. In our case, N is approximately 40. This is a rather large value and many transverse modes can take in the cavity. A crude estimate of the number of these modes can be made from mode volume considerations [26]. If we designate by V_{00} the active volume of the fundamental mode TEM_{00} in the cavity and by V_{mn} the active volume of the highest possible transverse mode TEM_{mn} , the approximate relationship holds :

$$V_{mn}/V_{00} = [(2m + 1)(2n + 1)]^{1/2}$$

With a fundamental mode volume V_{00} of about $\lambda\ell^2/2$ and considering that the highest mode occupies nearly the entire active volume, the ratio V_{mn}/V_{00} is of the order of 200. This shows that actually a very high number of transverse modes are present in the C.O.I.L. cavity. However, these modes are unlikely to be well defined in practice. Very small changes in the mirror alignment result in exchange of modes of different symmetries [26]. This has been observed experimentally, where, for the same laser power and running conditions, the overall laser beam profile can be completely different from run to run. This last observation confirms the high number of modes in the C.O.I.L.

A direct consequence of this mode multiplicity is that the eigenfrequencies of the resonator form almost a continuum, so that the laser oscillation takes place over the whole gain profile of the medium, without any narrowing due to a resonator selectivity. We have checked that the laser oscillates only on the $F^* = 3 \rightarrow F = 4$ hyperfine transition of the highest gain, with a total linewidth $\Delta\nu$ of 200 MHz, lower than the full width at half maximum of the Doppler broadening (250-300 MHz). Then only a part of the excited iodine atoms do participate to the gain. So in our model only the Doppler population within the ± 100 MHz interval around the maximum are taken into account in every step of the calculations. We have admitted that the various collisions which rearrange the translational velocities are sufficiently fast to maintain a Doppler distribution everywhere in the cavity.

3. Modeling of the laser.

In a first step, we have used a model similar to the one developed previously in the case of laser powers of a few watts [17]. After a brief description of the main features of this model, we will show that the calculated predictions systematically overestimate the laser power, so that this simple model becomes inadequate. In a second step, the model has been improved by the introduction of temperature effects which leads to a good agreement between expected and observed laser powers.

3.1 FIRST MODEL. — The basic assumption of the model is that the stimulated emission rate W is taken as constant throughout the active medium. This hypothesis results from the observed properties of the laser beam. First, this beam is uniform in power in any cross-section. It must be the same inside the resonator, i.e. . the electromagnetic power density must be constant everywhere in the active medium. Secondly, since the observed laser linewidth is 200 MHz, the gain laser medium appears to be inhomogeneous and all the active 200 MHz width gain profile participates in the laser oscillation. These two properties lead us to take a constant stimulation rate W for the $F^* = 3$ iodine level. Since the gain is equal to losses in every round trip in the laser cavity, W can be taken as :

$$W = \frac{A_{34} c^2 P}{8 \pi h \nu^3 \Delta \nu H (X_2 - X_1)} \frac{2 - a - t}{t} \quad (1)$$

where c is the speed of light, h Planck's constant, $\nu = 2.2794 \times 10^{14}$ Hz [25, 27] the frequency of the laser transition, with $\Delta \nu = 200$ MHz and $A_{34} = 5.1 \text{ s}^{-1}$ [27] the related Einstein coefficient. H and $(X_2 - X_1)$ are the active dimensions of the laser cavity cross-section (see Fig. 1) ; a and t are respectively the absorption and transmission coefficients of the two mirrors, and P is the laser output power.

The model describes the kinetics in two distinct regions :

- the flame of length X_1 from the I_2 injector to the beginning of the laser cavity, where the dissociation of I_2 occurs ;
- the laser cavity, where the molecular iodine concentration is very low.

In the first region, the change in the concentrations $[M_i]$ of the gas constituents is calculated from the rate equations :

$$\frac{d[M_i]}{dt} = \sum_i K_i [M_i] \quad (2)$$

where $[M_i]$ stands for the concentration of a given species [O_2^* , $I \dots$] at a distance X from the point of iodine injection, with the rate constants K_i reported in table I ($1 \leq K_i \leq 28$) and $dt = dX/V$, where V is the gas flow velocity. As the flow speed is rather low, we have admitted that the length for homogeneous mixing of the I_2 flow with the gases, is negligible with respect to X_1 . In the second region, of length $X_2 - X_1$, we add to the rate equations (2) the constant stimulated emission rate W (relation (1)) for the $F^* = 3$ level and the hyperfine relaxation rates (Tab. I, $29 \leq K_i \leq 33$). Since the lasing transition is between the hyperfine sublevels $F^* = 3(^2P_{1/2})$ and $F = 4(^2P_{3/2})$, having the respective degeneracies of 7 and 9, a positive gain exists only if :

$$\frac{[^2P_{1/2}(F^* = 3)]}{7} \geq \frac{[^2P_{3/2}(F^* = 4)]}{9}$$

Table I. — Rate equations considered in the model, with the abbreviated notations : $O_2 = O_2(^3\Sigma_g^-)$, $O_2^* = O_2(^1\Delta_g)$, $O_2^{**} = O_2(^1\Sigma_g^+)$, $I = I(^2P_{3/2})$, $I^* = I(^2P_{1/2})$, $I_{(F)}$ or $I_{(F)}^*$ = hyperfine sublevel F of I or I^* , $I_{(S)} = \{I_{(1)} + I_{(2)} + I_{(3)}\}$, and I_2^\dagger = high vibrational levels of I_2 ground state. The rate constants K_i are in units of $\text{cm}^{3n} \text{molecule}^{-2n} \text{s}^{-1}$ with $n = 1$ or 2 according to the order of the reaction. ΔE is the exoergicity of the reaction.

Reactions	Rate constants	Ref.	ΔE
$O_2^* + I \rightarrow O_2 + I^*$	$K_1 = 7.8 \times 10^{-11}$	28 ^a	279
$O_2 + I^* \rightarrow O_2^* + I$	$K_2 = 2.7 \times 10^{-11}$	28	-279
$O_2^* + I^* \rightarrow O_2^{**} + I$	$K_3 = 8.2 \times 10^{-14}$	29	2364
$O_2^{**} + I_2 \rightarrow O_2 + 2I$	$K_4 = 4.0 \times 10^{-12}$	30 ^c	681
$O_2^* + I_2 \rightarrow O_2 + I_2^\dagger$	$K_5 = 7.0 \times 10^{-15}$	31	0
$O_2^* + I_2^\dagger \rightarrow O_2 + 2I$	$K_6 = 3.0 \times 10^{-10}$	31 ^b 1	3045
	$K_6 = 3.0 \times 10^{-11}$	31 ^b 2	3045
$I^* + I_2 \rightarrow I_2^\dagger + I$	$K_7 = 3.6 \times 10^{-11}$	32	0
$I_2^\dagger + O_2 \rightarrow I_2 + O_2$	$K_8 = 5.0 \times 10^{-11}$	31 ^b 2	7603
	$K_8 = 5.0 \times 10^{-12}$	31 ^b 1	7603
$I_2^\dagger + Ar \rightarrow I_2 + Ar$	$K_9 = 4.0 \times 10^{-12}$	31 ^b 1	7603
	$K_9 = 1.0 \times 10^{-14}$	31 ^b 2	7603
$O_2^{**} + I_2 \rightarrow O_2 + I_2^\dagger$	$K_{10} = 1.64 \times 10^{-11}$	31 ^c	5518
$O_2^{**} + H_2O \rightarrow O_2 + H_2O$	$K_{11} = 6.71 \times 10^{-12}$	33	13121
$O_2^* + H_2O \rightarrow O_2 + H_2O$	$K_{12} = 4.0 \times 10^{-18}$	34	7882
$I_2^\dagger + H_2O \rightarrow I_2 + H_2O$	$K_{13} = 3.0 \times 10^{-10}$	31	7603
$I^* + H_2O \rightarrow I + H_2O$	$K_{14} = 1.7 \times 10^{-12}$	35	7603
$I^* + Cl_2 \rightarrow ICl + Cl$	$K_{15} = 0.25 \times 10^{-14}$	36 ^d	603
$I^* + Cl_2 \rightarrow I + Cl_2$	$K_{16} = 0.55 \times 10^{-14}$	37 ^d	4953
$I_2 + Cl_2 \rightarrow 2 ICl$	$K_{17} = 1.0 \times 10^{-14}$	37	2260
$I^* + ICl \rightarrow I + ICl$	$K_{18} = 0.75 \times 10^{-11}$	37 ^e	7603
$I^* + ICl \rightarrow I_2 + Cl$	$K_{19} = 0.75 \times 10^{-11}$	37 ^e	2693
$ICl + Cl \rightarrow I + Cl_2$	$K_{20} = 8.0 \times 10^{-12}$	38	2650

Reactions	Rate constants	Ref.	ΔE
$\text{Cl} + \text{I}_2 \rightarrow \text{ICl} + \text{I}$	$K_{21} = 2.0 \times 10^{-10}$	32	4910
$\text{I}^* + \text{Cl} \rightarrow \text{I} + \text{Cl}$	$K_{22} = 1.5 \times 10^{-11}$	32	7603
$\text{O}_2^* + \text{O}_2 \rightarrow \text{O}_2^{**} + \text{O}_2$	$K_{23} = 2.7 \times 10^{-17}$	29	2643
$\text{O}_2^* + \text{wall} \rightarrow \text{O}_2 + \text{wall}$	$K_{24} = 10 \text{ s}^{-1}$	f	0
$\text{O}_2^{**} + \text{wall} \rightarrow \text{O}_2 + \text{wall}$	$K_{25} = 20 \text{ s}^{-1}$	39	0
$\text{I}^* + \text{wall} \rightarrow \text{I} + \text{wall}$	$K_{26} = 1.0 \text{ s}^{-1}$	39	0
$2 \text{I}^* + \text{wall} \rightarrow \text{I}_2 + \text{wall}$	$K_{27} = 1.0 \text{ s}^{-1}$	39	0
$\text{I}^* \rightarrow \text{I} + \text{h}\nu$	$K_{28} = 8.0 \text{ s}^{-1}$	27	0
$\text{I} + \text{I}_{(2)}^* \rightarrow \text{I}_{(3)}^* + \text{I}$	$K_{29} = 1.0 \times 10^{-9}$	40,41	0
$\text{I}_{(2)}^* + \text{O}_2 \rightarrow \text{I}_{(3)}^* + \text{O}_2$	$K_{30} = 1.9 \times 10^{-10}$	42	0
$\text{I}_{(2)}^* + \text{Ar} \rightarrow \text{I}_{(3)}^* + \text{Ar}$	$K_{31} = 1.4 \times 10^{-10}$	42	0
$\text{I}_{(4)} + \text{Ar} \rightarrow \text{I}_{(5)} + \text{Ar}$	$K_{32} = 2.1 \times 10^{-10}$	42	0
$\text{I}_{(4)} + \text{O}_2 \rightarrow \text{I}_{(5)} + \text{O}_2$	$K_{33} = 2.8 \times 10^{-10}$	42	0

- a) Calculated with $K_{10} = 2.9$ at 295 K ($= K_1/K_2$) and $K_7 = 2.7 \times 10^{-11}$ measured in reference [28].
- b) 1 is model 1, and 2 is model 2 defined in reference [31].
- c) From reference [33], $K_{10} + K_4 = 2.04 \times 10^{-11}$. From the determinations in reference [30], we have used $K_4 = 0.2(K_{10} + K_4)$ and we have admitted that for K_{10} all I_2 is going to I_2^+ .
- d) We select $K_{16} = 0.55 \times 10^{-14}$ from reference [36]: $\text{I}^+ + \text{Cl}_2 \rightarrow \text{ICl} + \text{Cl}^+$ and we admit that it stands for the whole reaction: $\text{I}^+ + \text{Cl}_2 \rightarrow \text{ICl} + \text{Cl}^+$ (or Cl). Then, from reference [36], we infer $K_{15} = 0.25 \times 10^{-14}$ ($= 0.8 \times 10^{-14} \cdot 0.55 \times 10^{-14}$).
- e) With the assumption that $K_{18} = K_{19}$, using $K_{18} + K_{19} = 1.5 \times 10^{-11}$ determined in reference [37].
- f) From this work, before the iodine injection.

With this threshold condition the model calculates the laser power iteratively, with P as the only parameter. Starting with an approximate entrance P_1 value (for instance the experimental value), the model calculates the consumption of O_2 ($^1\Delta_g$) and the resulting laser power P_2 . The iteration process is stopped when the calculated power P_n is equal to the entrance power P_{n-1} . These calculations are performed with a sampling ratio X_2/dX of the order of 25 000, which gives a sufficient numerical stability of the results.

A careful examination of the O_2^* signal at the cavity walls brings to our attention the importance of the deactivation process after I_2 injection. At the beginning, with clean walls, the deactivation constant ($\text{O}_2^* + \text{wall} \xrightarrow{K_{24}} \text{O}_2 + \text{wall}$) was found to be close to 10 s^{-1} . But after I_2 injection and running of the laser, we observed an important increase of K_{24} ($> 50 \text{ s}^{-1}$) that was independent of the nature of the walls (pyrex, teflon, plexiglass, ...). But if we stop the I_2 injection and continue to run the 50 % O_2^* flow in the cavity, we can observe a decrease in K_{24} . After 10-20 min, K_{24} was divided by 2, depending on the nature of the walls and the previous running time of the laser. It was evident that I_2 sticks to the walls when injected in the

flow and forms a thin layer of I_2 (or I) at the surface of the walls. This layer gives the high value of K_{24} . With our new cavity, we have verified that the concentration in O_2^* was not significantly changed upward the I_2 injection, but the wall losses downward were not easy to determine, because of the concentration variations with the reactions. With an SF_6 flow, in the running conditions of the laser, K_{24} was around 20 s^{-1} and slightly higher without SF_6 (see Sect. 4).

Table II shows the comparison between the predictions of the model and the experimental results obtained in two different conditions, namely with or without the addition of a buffer gas (SF_6) along the cavity walls. It is clear that the SF_6 buffer gas increases significantly the laser power, but in lesser extent than our model predicts. In both cases, the predictions overestimate the actual laser power. This means that for laser powers in the range of a few tens of watts, new effects such as temperature changes, which have been neglected at lower laser powers, need to be included in our model.

Table II. — Comparison of the experimental laser powers with the predictions of the first model, with and without addition of the buffer gas SF_6 . The values taken for the wall deactivation rate constants K_{24} to K_{27} and for the water vapor concentration are optimised, as explained further (Tab. III).

	Flow I_2 Rate (mole/s)	Flow Cl_2 Rate (mole/s)	Pressure (Torr)	Laser Power exp.(watts)	Laser Power theor.(watts)
without SF_6	$6.05 \cdot 10^{-6}$	$2.8 \cdot 10^{-3}$	0.76	18	27
with SF_6	$6.05 \cdot 10^{-6}$	$2.8 \cdot 10^{-3}$	0.86	30	36

3.2 SECOND MODEL INCLUDING TEMPERATURE EFFECTS. — A temperature rise has to be expected during the course of the reactions since the collisional process of the population inversion is exothermic [$O_2(^1\Delta_g)$ deactivation liberates 7882 cm^{-1} and $I(^2P_{3/2}) \rightarrow I(^2P_{1/2})$ requires only 7603 cm^{-1}] and various deactivation processes occur (see Tab. I). In our previous work, where the gas speed was relatively high (30 m/s), we have shown that the energy extraction for the laser effect is not complete, giving a low laser power ($\leq 5\text{ W}$); so the correlated thermal effect is negligible as confirmed by our model. At lower speed, the laser power reaches a 25-30 W level and temperature effects have to be considered.

We will show that a temperature increase of 100 K can explain why our model overestimates the output power. The calculation of the temperature effect is performed at each step dX in the gas flow. First, at the temperature T obtained in the preceding step we calculate the energetic balance of the different endo and exothermic reactions (Tab. I) corresponding to the variations $d[M_i]$ of the gas constituents given by the rate equations (2). Knowing the specific heat of the gases in the flow and their concentrations $[M_i]$, the temperature variation ΔT can be calculated, assuming that this temperature is homogeneous in each cross-section of the gas flow. Thus we have :

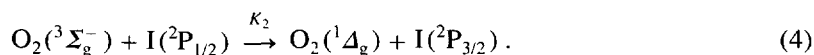
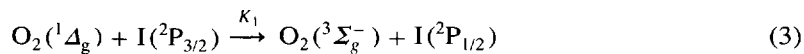
$$\Delta T = C_p^{-1} \sum_i \Delta E_i \cdot d[M_i],$$

where C_p is the specific heat capacity of the system and ΔE_i given in table I. To simplify calculations, C_p is assumed constant and from standard thermodynamical data, we have :

$$C_p = (7/2) R [O_2] + (8.3/2) R [H_2O] + (23.4/2) R [SF_6],$$

where R is the gas constant and $[O_2]$, $[H_2O]$ and $[SF_6]$ are the concentrations of the main species in the gas mixture. Then, the temperature for the next dX sample will be taken as $T + \Delta T$.

This procedure originates at the position of the iodine injection, where the temperature is assumed to be room temperature. The temperature changes throughout the flow, in the flame and in the laser cavity, and the variations of the rate constants with this temperature change have also to be considered. Among all the reactions given in the table I, the most important with respect to the laser effect are those leading to the population inversion in the iodine atoms, namely :



The reaction (3) having a small positive energy balance of 279 cm^{-1} is exothermic and K_1 is almost insensitive to a temperature variation. In contrast, the inverse reaction (4) requiring a collisional energy transfer from the medium is greatly enhanced by an increase of temperature, so that the rate constant K_2 is significantly temperature dependent. The ratio $K_e = K_1/K_2$ can be expressed as a function of the temperature T , provided that the equilibrium between the reactions (3) and (4) is reached. From standard thermodynamical calculations, the equilibrium constant K_e , defined by :

$$K_e = \frac{K_1}{K_2} = \frac{[O_2(^3\Sigma_g^-)] \cdot [I(^2P_{1/2})]}{[O_2(^1\Delta_g)] \cdot [I(^2P_{3/2})]}$$

can be written as :

$$K_e = \frac{g[O_2(^3\Sigma_g^-)] \cdot g[I(^2P_{1/2})]}{g[O_2(^1\Delta_g)] \cdot g[I(^2P_{3/2})]} e^{\frac{\Delta E}{kT}} \quad (5)$$

where $g[O_2(^3\Sigma_g^-)]$, $g[O_2(^1\Delta_g)]$, $g[I(^2P_{1/2})]$, and $g[I(^2P_{3/2})]$ are the degeneracies of the given states (equal to 3, 2, 2 and 4 respectively); ΔE is the exoergicity energy difference (279 cm^{-1}) and k the Boltzmann constant. K_e is given by the functional form :

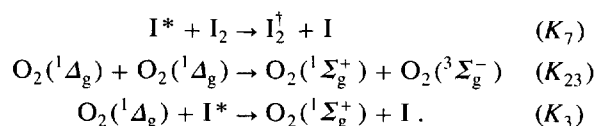
$$K_e = \frac{K_1}{K_2} = 0.75 \exp(402/T). \quad (6)$$

Several works have been devoted to the study of this temperature effect [30, 35, 43, 44]. From their results, we have adopted the value $K_1 = 7.8 \times 10^{-11} \text{ cm}^{-3} \text{ s}^{-1}$, and from equation (6) we have :

$$K_2 = 1.04 \times 10^{-10} \exp(-402/T).$$

A complete treatment of the temperature effect would include all the reactions summarized in the table I. Unfortunately very few of them have been studied.

Experimental data are available only for the three reactions :



The first reaction of the atomic iodine depopulation by I_2 can be described by an empirical equation [43, 46], of Arrhenius type :

$$K_7(T) = 3.89 \times 10^{-11} e^{\frac{835}{T}}$$

slightly different from that proposed by Kartasaev [47].

The second reaction of energy pooling between two $O_2(^1\Delta_g)$ molecules giving the highly excited state $O_2(^1\Sigma_g^+)$ has been studied for different temperature ranges (259 to 1 800 K) [35, 48] and we fitted the whole results with an empirical law :

$$K_{23}(T) = 7.0 \times 10^{-28} T^{3.8} e^{\frac{700}{T}}$$

The third reaction is very similar to the second one, being also an energy pooling mechanism giving the $O_2(^1\Sigma_g^+)$ state from the metastable state $O_2(^1\Delta_g)$. This is reflected by its rate constant K_3 which has been found to follow the same temperature law than K_{23} except for a scaling factor [35] :

$$\frac{K_3(T)}{K_{23}(T)} = (5.5 \pm 1.0) \times 10^3$$

To complete the description of the role played by the highly excited state $O_2(^1\Sigma_g^+)$ it is necessary to include the temperature effect on the iodine dissociation by $O_2(^1\Sigma_g^+)$ (K_4) and the deactivation of $O_2(^1\Sigma_g^+)$ by I_2 (K_{10}). Since the temperature law for these constants are unknown, we have assumed an empirical law of Arrhenius type :

$$K(T) = A \exp(\Delta E/kT),$$

where ΔE is the exoergicity and the constant A being calculated from the known K value at the room temperature. In this way we have taken :

$$K_4 = 1.44 \times 10^{-13} \exp(980/T)$$

$$K_{10} = 3.4 \times 10^{-23} \exp(7\,940/T).$$

The other rate constants of table I have been fixed at their room temperature values. Since the corresponding reactions are of relatively minor importance in the laser power, this approximation does not affect significantly the accuracy of our model. As will be shown below, this reduced set of temperature-dependent $K_i(T)$ rate constants gives us predictions in good agreement with the experimental data.

4. Results and discussion.

Apart from the temperature effects, the predictions of the model depend on the values taken for several parameters, mainly the wall deactivation, the water vapor concentration (about 1 %) and the $O_2(^1\Delta_g)$ concentration (about 50 % with 8-10 % accuracy). In order to have an idea of the error introduced by the uncertainty of these parameters we have calculated in tables III, IV and V the evolution of the theoretical laser power *versus* wall deactivations rates, water vapor concentration and $O_2(^1\Delta_g)$ concentration, respectively. Table III shows that the best choice for the wall deactivation effect is the set 20, 40, 2 and 2 s^{-1} for the K_{24} to K_{27} rate constants, with the SF_6 flow, when the water vapor concentration is taken to be 1 %. This table shows also that the laser power is rather sensitive to the choice of these parameters. Table IV related to the

Table III. — Predicted laser power as a function of wall deactivation rate constants, for two experimental conditions. (A) : $O_2(^1\Delta_g)$ concentration 48 %, water vapor concentration 1 %, SF_6 flow rate 2×10^{-3} mole s^{-1} , observed laser power 33.7 W. (B) : $O_2(^1\Delta_g)$ 46.9 %, H_2O 1 %, SF_6 2×10^{-3} mole s^{-1} , observed laser power 30.0 W. The best fit is clearly the set 20, 40, 2 and $2 s^{-1}$ for the K_{24} to K_{27} constants. Since only the first constant K_{24} has been measured to be around $20 s^{-1}$, the three others have been estimated from the given values of table I on a proportionality hypothesis. The same studies made in the case of the absence of the SF_6 flow, lead to the values of 25, 50, 2.5 and $2.5 s^{-1}$ for the K_{24} to K_{27} constants.

K_{24}	K_{25}	K_{26}	K_{27}	Exp. (A)	Exp. (B)
				Predicted Power	Predicted Power
				(watts)	(watts)
	s^{-1}				
10	20	1	1	43.3	41.0
20	40	2	2	35.4	32.2
30	60	3	3	28.7	25.0
Observed Power (watts)				33.7	30.

Table IV. — Predicted laser power as a function of water vapor concentration. The experimental conditions (A) and (B) are the same as those quoted in table II, K_{24} to K_{27} being 20, 40, 2 and $2 s^{-1}$ respectively. From experimental measurements, the H_2O relative concentration is about 1 %. This study also shows that an increase of a factor 2 in H_2O concentration decreases the laser power by only 10 %.

Water Vapor Concentration (%)	Experiment (A) Predicted Power (watts)	Experiment (B) Predicted Power (watts)
0.5	37.1	34.1
1.0	35.4	32.2
1.5	34.4	31.1
2.0	32.9	30.5
Observed Power (watts)	33.7	30.0

Table V. — Predicted laser power as a function of $O_2(^1\Delta_g)$ concentration. Experimental conditions are the same as in tables III and IV, H_2O concentration being 1 %. The optimum values of $O_2(^1\Delta_g)$ concentration are 48 % for A and 46 % for B, quite close to the measured values of 48.2 and 46.3 respectively. This study highlights the critical role of the $O_2(^1\Delta_g)$ concentration : an increase from 45 to 52 % increases the laser power from 30 to 40 W.

$O_2(^1\Delta_g)$ Concentration (%)	Experiment (A) Predicted Power (watts)	Experiment (B) Predicted Power (watts)
45	31.1	30.6
46	32.5	32.2
47	34.0	33.8
48	35.4	35.3
50	38.4	38.6
52	41.3	40.2
Observed Power (watts)	33.7	30.0

water vapor concentration confirms that our measured value of 1 % is realistic, but the decrease of the laser power for an increase from 0.5 to 2.0 % in water concentration is not very important. Table V shows the predicted laser power *versus* $O_2(^1\Delta_g)$ concentration. The good agreement between observed and calculated laser power at our measured $O_2(^1\Delta_g)$ concentration, confirms that both our measurement of $O_2(^1\Delta_g)$ is accurate [17] and our model gives realistic laser output power. This last study also shows that the laser power depends critically upon the $O_2(^1\Delta_g)$ concentration $\{ [O_2(^1\Delta_g)] / [O_2(^1\Delta_g) + O_2(^1\Sigma_g^+) + O_2(^3\Sigma_g^-)] \}$: an increase from 48 to 52 % of $O_2(^1\Delta_g)$ raises the laser power from 35 to 41 W.

Given suitable deactivation rates and water vapor concentration, the model gives the predicted laser power for given initial conditions. Table VI summarizes some experimental results together with the predictions of the model. In most of the experiments the temperature rise is around 100 K. It has to be noted that this temperature is close to the rotational temperature of I_2 in the flame region (from 0 to X_1 in Fig. 1), which has been measured elsewhere [49, 50]. Table VI shows clearly that the addition of the SF_6 buffer gas significantly increases both the output laser power and the chemical yield. The chemical yield is defined as the ratio of the measured laser power over the chemical power contained in the O_2 flow due to the 7881 cm^{-1} available energy of the $O_2(^1\Delta_g)$ molecule. This improvement is due in part to the reduction of deactivation on the walls, but the main effect is the reduction of the temperature of the active medium which allows a better extraction of the laser power.

Table VI. — Summary of some experimental results, together with predictions from the model. The wall losses (K_{24} to K_{27} rate constants of Tab. I) are 25, 50, 2.5 and 2.5 s^{-1} without SF_6 and 20, 40, 2 and 2 s^{-1} with SF_6 . The H_2O concentration is 1%. The chemical yield is defined as the ratio of the measured laser power over the chemical power contained in the O_2 flow due to the 7881 cm^{-1} available energy of the $\text{O}_2(^1\Delta_g)$ molecule. These results show clearly that, without SF_6 , low laser powers are correlated to high gas temperature, while the addition of SF_6 gives high laser powers and low temperature increases, illustrating the cooling effect of the buffer gas. For each run with SF_6 , the SF_6 flow rate has been optimised for the maximum laser power. This gives almost the same value of $2 \times 10^{-3} \text{ mole s}^{-1}$ for the SF_6 flow rate in all the experiments.

I_2	Cl_2	Measured $\text{O}_2(^1\Delta_g)$ Concentration	Pressure	SF_6	Initial Flow Speed	Measured Power	Calculated Power	ΔT	Chemical Yield
($\mu \text{ mole/s}$)	(m mole/s)	(%)	(Torr)	(m mole/s)	(m/s)	(watts)	(watts)	(K)	(%)
7.60	2.35	44	0.70	0.0	7.9	15.0	15.0	330	6.7
6.05	2.20	47	0.71	2.0	8.8	27.0	27.6	74	12.8
6.05	2.80	46	0.76	0.0	8.6	18.0	17.8	363	6.8
6.05	2.80	46	0.86	2.0	8.3	30.0	32.2	93	11.4
8.56	2.08	47	0.61	0.0	8.0	17.0	16.8	330	8.7
8.56	2.08	47	0.69	1.9	8.6	25.6	27.7	76	13.1
8.56	2.70	48	0.91	2.0	7.7	33.7	35.4	103	13.2

In fact, our model shows that all the available energy is extracted in the flow before the end of the laser cavity. This confirms the predictions derived in our previous work [17], in which the flow speed was too high to allow a complete power extraction. In our present design, this flow speed has been reduced, so that the hyperfine and translational relaxation rates, which statistically populate the upper laser level and deplete the lower one through collisions, are sufficiently fast to compete with the disequilibrium in $F^* = 3$ and $F = 4$ populations produced by the stimulated emission process. As a consequence, all the excited iodine atoms release their energy *via* the $F^* = 3 \leftarrow F = 4$ transition, with an extraction length lower than $(X_2 - X_1)$. But finally, due to the mode symmetry, the laser oscillates on the whole cavity length $(X_2 - X_1)$. Thus we can consider that the limit of the power extraction is governed by the degeneracies of the fine structure levels $\text{I}(^2\text{P}_{1/2})$ and $\text{I}(^2\text{P}_{3/2})$ with the corresponding threshold $[\text{O}_2(^1\Delta_g)]/[\text{O}_2(^3\Sigma_g^-)]$ of 0.171 at room temperature.

One would expect that the chemical yield depends critically upon the ratio of active species I_2 and $\text{O}_2(^1\Delta_g)$. Our experimental determinations as well as the model show that this optimum ratio and the corresponding chemical yield depend also on whether a buffer gas is added or not. As can be seen in figure 2, the optimum molar ratio without the buffer gas is around 0.5% for a chemical yield of 7-8%, and with a SF_6 flow, the same quantities are around 0.8% and 12-13%, respectively.

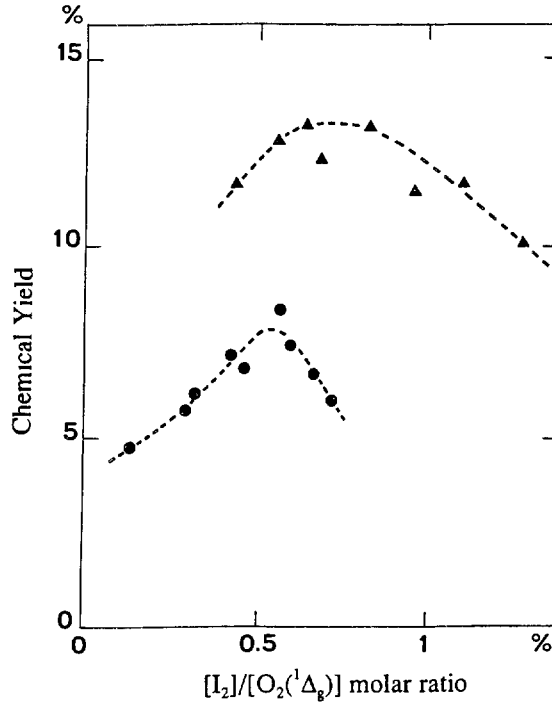


Fig. 2. — Chemical yield as a function of the ratio of the I_2 concentration over the $O_2(^1\Delta_g)$ concentration. The chemical yield is defined as the ratio of the obtained laser power over the chemical power contained in the oxygen flow. Dots correspond to experiments without SF_6 and triangles correspond to experiments with SF_6 flow.

Since the model and the experimental results are in good agreement, it is possible in principle to estimate the optimum conditions of the laser running for a given pumping system. In fact, this could be rather difficult since the behaviour of the laser power depends of numerous parameters sometimes not easy to determine quantitatively. The best running conditions have to be determined iteratively in a given range of the initial parameter values.

5. Conclusion.

We have shown that our model, taking into account the temperature effects, properly calculates the expected power of a C.O.I.L., for given running conditions at power up to 30 W. The most important result is that the adding of an inert buffer gas such as SF_6 has considerably increased the laser power. This increase is mainly due to a cooling of the active medium which favours a better laser power extraction. From these results we can say that, at least for a subsonic C.O.I.L. device, the presence of a buffer gas is necessary to achieve a good energy extraction from the laser medium. This necessity becomes less obvious in the case of a supersonic device in which a significant cooling of the medium is achieved by the isentropic expansion of the gases.

Acknowledgments.

The authors would like to acknowledge their debt to Professor R. Bacis for his help and numerous and fruitful discussions all along this work.

This work was supported by the Direction des Recherches, Etudes et Techniques (D.R.E.T.) and the Centre National de la Recherche Scientifique (C.N.R.S.), France.

References

- [1] McDermott W. E., Pchelkin N. R., Benard D. J. and Bousek R. R., An electronic transition chemical laser, *Appl. Phys. Lett.* **32** (1978) 469-470.
- [2] Benard D. J., McDermott W. E., Pchelkin N. R. and Bousek R. R., Efficient operation of a 100 W transverse-flow oxygen-iodine chemical laser, *Appl. Phys. Lett.* **34** (1979) 40-41.
- [3] Richardson R. J. and Wiswall C. E., Chemically pumped iodine laser, *Appl. Phys. Lett.* **35** (1979) 138-139.
- [4] Bachar J. and Rosenwaks S., An efficient, small scale chemical oxygen-iodine laser, *Appl. Phys. Lett.* **41** (1982) 16-18.
- [5] Miller D. J., Clendening C. W., English W. D., Berg J. G. and Trost J. E., « 1 kW C.W. chemical oxygen iodine laser », F S2, CLEO 82, Conference on Lasers and Electro-Optics, Phoenix, AZ (Optical Society of America, Washington DC., 1982) p. 170.
- [6] Watanabe K., Kashiwabara S., Sawai K., Toshima S. and Fujimoto R., Performance characteristics of a transverse-flow oxygen-iodine chemical laser in a low gas-flow velocity, *J. Appl. Phys.* **54** (1983) 1228-1231.
- [7] Watanabe K., Kashiwabara S., Sawai K., Toshima S. and Fujimoto R., Small-Signal Gain and Saturation Parameter of a Transverse-Flow CW Oxygen-Iodine Laser, *IEEE J. Quantum Electron.* **QE19** (1983) 1699-1703.
- [8] Bonnet J., David D., Georges E., Leporcq B., Pigache D. and Verdier C., Experimental analysis of a chemical oxygen-iodine laser, *Appl. Phys. Lett.* **45** (1984) 1009-1011.
- [9] Wiswall C. E., Lilienfeld H. W. and Bragg S., Operation of an ICl fueled oxygen-iodine laser, *Appl. Phys. Lett.* **45** (1984) 5-7.
- [10] Vagin N. P., Konosheko A. F., Kryukov P. G., Nurligareev D. Kh., Pazyuk V. S., Tomashov V. N. and Yuryshv N. N., Chemical oxygen-iodine laser utilizing low-strength hydrogen peroxide, *Sov. J. Quantum Electron.* **14** (1984) 1138-1139.
- [11] Watanabe K., Mutoh M., Kashiwabara S. and Fujimoto R., « Theoretical Modeling and Analyses of Chemically Pumped, C.W. Iodine Laser Oscillators », Proceedings of the Fifth International Symposium on Gas Flow and Chemical Lasers, A. S. Kaye and A. C. Walker Eds., *Inst. Phys Conf. Ser.* No. 72 (Hilger, London, 1985) pp. 181-186.
- [12] Wiswall C. E., Bragg S. L., Reddy K. V., Lilienfeld H. V. and Kelley J. D., Moderate-power C.W. chemical oxygen-iodine laser capable of long duration operation, *J. Appl. Phys.* **58** (1985) 115-118.
- [13] Watanabe K., Kashiwabara S. and Fujimoto R., Efficiency of chemical oxygen-iodine lasers : Theoretical simulation and experiment, *J. Appl. Phys.* **59** (1986) 42-48.
- [14] Yoshimoto H., Yamakoshi H., Shibukawa Y. and Uchiyama T., A highly efficient, compact chemical oxygen-iodine laser, *J. Appl. Phys.* **59** (1986) 3965-3967.
- [15] David D., Georges E., Leporcq B., Pigache D. and Verdier C., « Theoretical Modelling and Experimental Analysis of Chemical Oxygen-Iodine Lasers », Proceedings of the Sixth International Symposium on Gas Flow and Chemical Lasers, S. Rosenwaks Ed., Springer Proceedings in Physics 15 (Springer, Berlin, 1986) pp. 170-177.
- [16] Bacis R. and Churassy S., « Chemical Oxygen-Iodine Laser Mechanisms and High Resolution Spectroscopy Studies », Proceedings of the Sixth International Symposium on Gas Flow and Chemical Lasers, S. Rosenwaks Ed., Springer Proceedings in Physics 15 (Springer, Berlin, 1986) pp. 142-155.
- [17] Churassy S., Bacis R., Bouvier A. J., Pierre C. dit Mery C., Erba B., Bachar J. and Rosenwaks S., The chemical oxygen-iodine laser : comparison of a theoretical model with experimental results, *J. Appl. Phys.* **62** (1987) 31-35.
- [18] Basov N. G., Kryukov P. G. and Yuryshv N. N., Pulse-periodic operation of an oxygen-iodine chemical laser, *Sov. J. Quantum Electron.* **17** (1987) 588-594.

- [19] Yoshida S., Endoh M., Sawano T., Amano S., Fujii H. and Fujioka T., Chemical oxygen iodine laser of extremely high efficiency, *J Appl Phys.* **65** (1989) 870-872.
- [20] a) Yoshida S., Fujii H., Amano S., Endoh M., Sawano T. and Fujioka T., Development of Chemical Oxygen Iodine Lasers for industrial uses. 7th International Symposium on Gas Flow and chemical lasers (Vienna, 22-26 August 1988), D. Schuocker ed., *Proceeding Spie* **1031** (1989) 282-286 ;
- b) Kikuchi T., Tsuruyama T. and Uchiyama T., Performance characteristics of a chemical oxygen-iodine laser without a water vapor trap, *ibid* 287-293 ;
- c) Igoshin V. I. and Zaikin A. P., About controlling and changing pulse length of chemical oxygen-iodine laser, *ibid* 301-305.
- [21] a) Avizonis P. V., Hansen G. A. and Truesdell K. A., The Chemically-Pumped Oxygen Iodine Laser, High-Power Gas Lasers (Los Angeles, 15-17 January 1990), P. V. Avizonis, C. Freed, J. J. Kim, F. K. Tittel Eds. *Proceedings Spie* **1225** (1990) 448-476 ;
- b) Yoshida S. J. and Shimizu K., High power chemical oxygen iodine laser for industrial applications, *ibid.* 478-481 ;
- c) Highland R., Crowell P. and Hager G., A 630 W average power Q-switched chemical oxygen-iodine laser, *ibid.* 512-520.
- [22] a) Yoshida S. and Shimizu K., High power chemical oxygen iodine lasers and applications. 8th International symposium on Gas Flow and Chemical lasers (Madrid, 10-14 September 1990), J. M. Orza and C. Domingo Eds., *Proceedings Spie* **1397** (1991) 205-212 ;
- b) Fujii H., Iizuka M., Muro M., Huchiki H. and Atsuta T., Development of chemical oxygen-iodine laser for industrial application, *ibid* 213-220 ;
- c) Yuryshch N. N., Pulsed Chemical Oxygen-Iodine Laser, *ibid* 221-230 ;
- d) Barnault B., Barraud R., Forestier L., Georges E., Louvet Y., Mouthon A., Ory M. and Pigache D. R., A high power chemical oxygen-iodine laser, *ibid* 231-234 ;
- e) Bohn W. L., Truesdell K. A., Latham W. P. and Avizonis P. V., Small signal gain in the oxygen-iodine laser, *ibid* 235-238 ;
- f) Matsuzaka F., Nigawara K., Terasawa K. and Uchiyama T., Second harmonic generation of chemical oxygen iodine laser, *ibid.* 239-242.
- [23] Schmiedberger J., Kodymova J., Kovar J., Spalek O. and Tenda P., Magnetic modulation of gain in a chemical oxygen-iodine laser, *IEEE J. Quant Elect* **27** (1991) 1262-1264.
- [24] a) Bohn W. L. The chemical oxygen-iodine laser : achievements, problems and future perspectives. 9th International Symposium on Gas Flow and Chemical Lasers (Heraklion, Crete, 21-25 September 1992), C. Fotakis, C. Kalpouzos, T. Papazoglou Eds., *Proceedings Spie* **1810** (1992) 468-475 ;
- b) Truesdell K. A., Lamberson S. L. and Hager G. D., Phillips Laboratory C.O.I.L. Technology Overview, *ibid* 476-492 ;
- c) Bouvier A. J., Bacis R., Bouvier A., Cerny D., Churassy S., Crozet P. and Nota M., On the dissociation of molecular iodine by singlet molecular oxygen in the chemical oxygen iodine laser : Spectroscopy and role of the lower excited states and two non radiative reservoir states, *ibid* 493-496 ;
- d) Fujii H., Wani F., Muro M. and Atsuta T., Performance of chemical oxygen iodine laser for industrial application, *ibid* . Wd FP4 (unpublished) ;
- e) Eroshenko V. A., Kalinovski V. V., Kirillov G. A., Kononov V. V. and Nikolaev V. D., Experimental and theoretical investigation of oxygen-iodine laser with the power up to 5 kW, *ibid* . Wd FP6 (unpublished).
- f) Kulagin Yu., Shelepin L. A. and Yarygina V. N., Search of optimal conditions for the atomic iodine generation feasibility. *ibid.*, Wd FP7 (unpublished).
- g) Frolov M. P., Ishkov P. V., Kryukov P. G., Pasyuk V. S. and Yuryshch N. N., Visible chemical oxygen-iodine laser based on the second harmonic generation, *ibid.*, Wd FP9 (unpublished).
- h) Hager G. D., Kopf D., Plummer D. N., Salsilp T. and Crowell P. G., Demonstration of a Repetively Pulsed Magnetically Gain Switched Chemical Oxygen Iodine Laser, *ibid.* 509-512 ;

- i) Barmashenko B. D., Elmor A., Lebiush E. and Rosenwaks S., The effect of mixing on iodine dissociation, population inversion and lasing in chemical oxygen-iodine lasers, *ibid.* 513-516 ;
- j) Dvoryankin A. N., Two-dimensional modeling of the chemical oxygen iodine laser, *ibid.*, Wd FP12 (unpublished) ;
- k) Schmiedberger J., Spalek O., Kodymova J. and Kovar J., Experimental study of magnetic quenching of laser generation in C.O.I.L., *ibid.* 521-524 ;
- l) Pigache D., Georges E. and Louvet Y., Theoretical and experimental analysis of a Chemical Oxygen Iodine Laser, *ibid.* 528-531 ;
- m) Miura N., Mese N., Yoshino S. and Uchimaya T., Second Harmonic Generation of Chemical Oxygen Iodine Laser, *ibid.* 536-539.
- [25] Koenig E. L., Morillon C. and Verges J., Etude de la Transition « Interdite » ${}^3P_{1/2} \rightarrow {}^3P_{3/2}$ de la Configuration np^5 dans le brome et l'iode par Spectrométrie de Fourier, *Physica* **70** (1973) 175-189.
- [26] Röss D., Lasers-Light Amplifiers and Oscillators (Academic Press, 1969) pp. 204-207.
- [27] Brederlow G., Fill E. and Witte K. J., The High-Power Iodine Laser (Springer, Berlin, 1983) pp. 4-22.
- [28] Young T. and Houston P. L., The $I({}^2P_{1/2}) + O_2 \rightleftharpoons I({}^2P_{3/2}) + O_2({}^1\Delta)$ equilibrium, *J. Chem. Phys.* **78** (1983) 2317-2326.
- [29] Lilienfeld H. V., Carr P. A. G. and Hovis F. E., Energy pooling reactions in the oxygen-iodine system, *J. Chem. Phys.* **81** (1984) 5730-5736.
- [30] Muller D. F., Young R. H., Houston P. L. and Wiesenfeld J. R., Direct observation of I_2 collisional dissociation by $O_2(b^1\Sigma_g^+)$, *Appl. Phys. Lett.* **38** (1981) 404-406.
- [31] Heidner III R. F., Gardner C. E., Segal G. I. and El-Sayed T. M., Chain-Reaction Mechanism for I_2 Dissociation in the $O_2({}^1\Delta)$ -I Atom Laser, *J. Phys. Chem.* **87** (1983) 2348-2360.
- [32] Burde D. H. and McFarlane R. A., Collisional quenching of excited iodine atoms $I(5p^5\ ^2P_{1/2})$ by selected molecules, *J. Chem. Phys.* **64** (1976) 1850-1851.
- [33] Aviles R. G., Muller D. R. and Houston P. L., Quenching of laser-excited $O_2(b^1\Sigma_g^+)$ by CO_2 , H_2O and I_2 , *Appl. Phys. Lett.* **37** (1980) 358-360.
- [34] Becker K. H., Groth W. and Schurath U., The Quenching of Metastable $O_2({}^1\Delta_g)$ and $O_2({}^1\Sigma_g^+)$ molecules, *Chem. Phys. Lett.* **8** (1971) 259-262.
- [35] Heidner III R. F., Gardner C. E., El-Sayed T. M., Segal G. I. and Kasper J. V. V., Temperature dependence of $O_2({}^1\Delta) + O_2({}^1\Delta)$ and $I({}^2P_{1/2}) + O_2({}^1\Delta)$ energy pooling, *J. Chem. Phys.* **74** (1981) 5618-5626.
- [36] Hall G. E., Arepalli S., Houston P. L. and Wiesenfeld J. R., Collisional quenching of excited iodine atoms ($5p^5\ ^2P_{1/2}$) by Cl_2 in a flow system, *J. Chem. Phys.* **82** (1985) 2590-2597.
- [37] Lilienfeld H. V., Whitefield P. D. and Bradburn G. R., $I({}^2P_{1/2})$ Deactivation by ICl and Cl_2 , *J. Phys. Chem.* **88** (1984) 6158-6162.
- [38] Clyne M. A. A. and Cruse H. W., Atomic Resonance Fluorescence Spectrometry for the Rate Constants of Rapid Bimolecular Reactions, *J. Chem. Soc. Faraday II* **68** (1972) 1377-1387.
- [39] Fisk G. A. and Hays G. N., Kinetic rates in the oxygen-iodine system, *J. Chem. Phys.* **77** (1982) 4965-4971.
- [40] Katulin V. A., Nosach V. Yu. and Petrov A. L., Investigation of the characteristics of the preamplifier of a short-pulse iodine laser, *Sov. J. Quantum Electron.* **9** (1979) 169-174.
- [41] Yukov E. A., Elementary processes in the active medium of an iodine photo dissociation laser, *Sov. J. Quantum Electron.* **3** (1973) 117-120.
- [42] Cerny D., Bacis R., Bussery B., Nota M. and Vergès J., Experimental determination and calculation of the collision relaxation rates in the $5^2P_{1/2}$ and $5^2P_{3/2}$ levels of atomic iodine, *Chem. Phys.* **95** (1991) 5790-5798.
- [43] Lilienfeld H. V., Carr P. A. G. and Hovis F. E., Investigation of the Temperature Dependence of the Excitation Mechanism of the Oxygen-Iodine Chemical Laser, *Chem. Phys. Lett.* **93** (1982) 38-42.
- [44] Joly V., Etude Théorique et Expérimentale des Mécanismes Cinétiques dans le Laser Iode-Oxygène Chimique (LIOC), Thesis, Paris Sud Orsay (1989).

- [45] Derwent R. G. and Thrush B. A., The radiative lifetime of the metastable iodine atom $I(5^2P_{1/2})$, *Chem. Phys Lett* **9** (1971) 591-592.
- [46] Deakin J. J. and Husain D., Temperature Dependence of Collisionally induced Spin Orbit Relaxation of Electronically Excited Iodine Atoms, $I(5p^2\ ^2P_{1/2})$, *J. Chem. Soc Faraday II* **68** (1972) 1603-1612.
- [47] Kartashev V. A., Penkin N. P. and Tolmachev Yu. A., Determination of the temperature dependence of the rate constant representing quenching of metastable iodine atoms by iodine molecules, *Sov J Quantum Electron.* **7** (1977) 608-610.
- [48] Borrell P. M., Borrell P., Grant K. R. and Pedley M. D., Rate Constants for the Energy-Pooling and Quenching Reactions of Singlet Molecular Oxygen at High Temperatures, *J Phys Chem* **86** (1982) 700-703.
- [49] Cerny D., Bacis R., Bouvier A. J., Poulat S., Topouzkhanian A. and Vergès J., The dissociation of molecular iodine by metastable oxygen. I. Populations of Alu and BO_v^+ iodine states through Fourier Transform Spectrometry, *J.Q.S.R.T.* **47** (1992) 9-18.
- [50] Bouvier A. J., Bacis R., Bouvier A., Cerny D., Churassy S., Crozet P. and Nota M., The dissociation of molecular iodine by metastable oxygen. II. Populations of reservoir states through laser excitation spectra. *J.Q.S.R.T.* **49** (1993) 311-323.